Large and Giant Vesicles "Decorated" with Chitosan: Effects of pH, Salt or Glucose Stress, and Surface Adhesion

Francois Quemeneur,[†] Ayman Rammal,[†] Marguerite Rinaudo,[‡] and Brigitte Pépin-Donat*[,†]

Laboratoire Electronique Moléculaire Organique et Hybride/UMR 5819 SPrAM (CEA-CNRS-UJF)/DRFMC/ CEA-Grenoble, 38054 Grenoble Cedex 9, France, and Centre de Recherches sur les Macromolecules Végétales (CERMAV-CNRS) affiliated with Joseph Fourier University, BP53, 38041 Grenoble Cedex 9, France

Received December 27, 2006; Revised Manuscript Received June 1, 2007

This paper describes the behavior of large and giant unilamellar vesicles (LUVs and GUVs, respectively) in the presence of chitosan, a positively charged polyelectrolyte. Variation of the ζ-potential of LUVs as a function of chitosan concentration is studied for two different molecular weights (MW) after a preliminary study devoted to pH and salt effects on ζ-potential in order to discriminate among the effects of protons, salt, and chitosan concentrations. The difference observed between pH and salt effects on the one hand and chitosan on the other allows us to conclude there is a strong LUV−chitosan interaction. In presence of chitosan, the ζ-potential of LUVs becomes positive and two distinct regimes of variation are suggested and interpreted as follows: a first step consists of chitosan adsorption flat on the membrane (independent of MW) followed by a possible reorganization of the polymer of higher molecular weight on the surface, giving rise to loops. Then a comparative observation of the effect of pH and salt by optical microscopy is made on naked and chitosan-decorated GUVs. Results further confirm a membrane-chitosan interaction and are interpreted in the light of the results obtained for LUVs in terms of both electrostatic and hydrophobic interaction. A large majority of decorated vesicles remain stable down to pH = 1 while in the absence of chitosan they burst quickly at pH between 2 and 3. Osmotic pressure and net charge change due to addition of HCl results in a decrease in the diameter of the decorated vesicles, which remain spherical while forming tubes of lipids. In presence of NaCl, a higher resistance of decorated vesicles is also evidenced (they are stable for NaCl concentrations up to 10^{-1} M while naked vesicles burst when [NaCl] is between 10^{-2} and 10^{-3} M). At higher salt concentration, aggregation of decorated vesicles occurs, which is attributed to the screening of electrostatic repulsions between vesicles covered by the positively charged chitosan. Finally, adhesion of vesicles on a positively charged surface is investigated. In absence of chitosan, the vesicles immediately burst when they come in contact with the surface. On the contrary, suspension of chitosan-vesicles remain stable down to pH = 1.5. Under gentle flow vesicles move: they do not adhere on the substrate, probably due to the repulsion between positively adsorbed charged chitosan and substrate; spherical deflation occurs, but in this case daughter vesicles are formed instead of lipid tubes.

Introduction

Liposomes are made of self-closed phospholipid bilayers or multilayers and are respectively referred to as unilamellar and multilamellar vesicles. Their diameter varies between a few nanometers and hundred micrometers. Giant unilamellar or multilamellar vesicles (respectively GUVs and GMVs) exhibit a diameter of 0.5 μm < d < 100 μm. They present the advantage of being directly observable by optical microscopy and are generally studied as the simplest cell model.[1] Small unilamellar or multilamellar vesicles (respectively SUVs and SMVs) (20 nm < d < 100 nm) and large unilamellar or multilamellar vesicles (LUVs and LMVs) (100 nm < d < 500 nm) are often studied as protective capsules[2−6] and used as efficient drug carriers for a large panel of compounds like vaccines, diagnostic agents, and proteins.[7−16]

Lipid layers, which form the membrane of living cells, are often "decorated" by macromolecules such as proteins and glycoconjugates. Interaction between these macromolecules and membranes may give rise to changes in cell behavior. For example, the carbohydrate-rich layer called the glycocalyx,[17] which surrounds some living cells, modifies cell−cell or cell−surface interaction. Therefore, it is of interest to study changes in membrane properties and in behavior of GUVs upon interaction with anchored and/or adsorbed polymers under external stresses. Actually, complex vesicle shape changes upon interaction with macromolecules (such as budding, pearling, and coiling) are reported extensively in the literature.[18−23] As far as SUV and LUV protective capsules are considered, it is of interest to study the effect of decoration by polymers on their resistance to the in vivo environment, absorption properties, and specificity toward targets. For example, LUVs were covered or grafted with polyethylene glycol in order to make them furtive and stable in the intravenous environment.[9,24,25] Then chitosan, a pseudonatural macromolecule derived from chitin, the main organic component of crustacean shells, cuticles of insects, and cell walls of some fungi,[26,27] was proposed as an alternative to polyethylene glycol[9] because of its biocompatibility and biodegradability[28−32] and of its properties of specific adsorption such as mucoadhesive properties.[33]

* Corresponding author. Tel: 00 33 4 38 78 38 06. Fax: 00 33 4 38 78 51 13. E-mail: Brigitte.pepin-donat@cea.fr.

[†] Laboratoire Electronique Moléculaire Organique et Hybride.

[‡] Centre de Recherches sur les Macromolecules Végétales (CERMAV-CNRS).

10.1021/bm061227a CCC: $37.00
Published on Web 07/21/2007

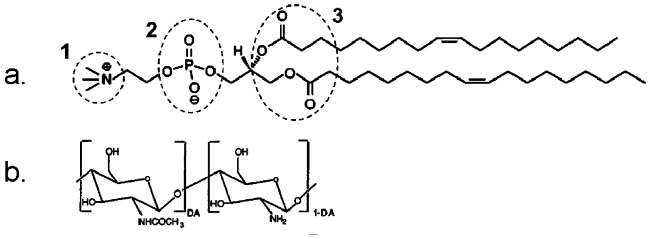

Figure 1. Structure of the chemical products used during this study. (a) 1,2-Dioleoyl-*sn*-glycero-3-phosphocholine (DOPC) with the following active sites: the polar head group with a positive quaternary amino group (1), a negative phosphate group (2), and two "carbonyl oxygen" groups (3), which connect hydrophilic head group and the two hydrophobic tails. (b) Two constitutive units of chitosan.

Chitosan is a linear copolymer of β-(1→4)-D-glucosamine and β-(1→4)-*N*-acetyl-D-glucosamine, which is insoluble in neutral and basic media but becomes soluble in slightly acidic medium (pH < 6) due to the protonation of the amine functions. This solubility allows thus its coprocessing with other biomolecules based on polyelectrolyte complex formation.[34] Then, the positively charged backbone of chitosan (the charge of which can be controlled by pH) is determinant for its interaction with other macromolecules and supramolecular architectures.[35]

The effect of chitosan on dipalmitoyl-*sn*-glycero-3-phosphocholine (DPPC) GMVs was showed to result in an alteration of their membrane structure, which was attributed to the insertion of chitosan into their membranes during their formation.[36] Physical driving forces (mostly of electrostatic origin) were studied by observation of the interaction of phospholipid vesicles with immobilized chitosan on amino-silanized glass.[37,38] The effect of chitosan on soybean phosphatidylcholine LMVs prepared by inverse phase was also reported; in this case, chitosan is present both on the inner and the outer surfaces of the membrane.[28,39]

We focus in this paper on both GUVs and related LUVs obtained by extrusion of these GUVs. We report successively the effect of decoration by chitosan (on the outer side of the membrane) on the behavior of LUVs and GUVs under different kinds of external stresses due to salt, pH or glucose shocks, and adhesion on a positively charged surface.

Materials and Methods

Materials. *Lipid* 1,2-dioleoyl-*sn*-glycero-3-phosphocholine (DOPC, Figure 1a) (MW = 786.15) is purchased from Avanti Polar Lipids and dissolved as received in a chloroform/methanol solution (9/1 volume ratio) at 2 mg/mL.

Highly purified 18.2 MΩ.cm water is used for the preparation of all the solutions.

Chitosan is obtained from Far East crab shells by the method of Mullagaliev[40] (Figure 1b). Its degree of acetylation (DA) is equal to 5% and its weight-average molecular weight (Mw) is equal to 225 000. Another sample with MW = 50 000 and DA = 4.1% from shrimps is provided by Primex. The solution of chitosan used for vesicles incubation is prepared at 1 g/L by dissolving the polymer in 10 mL of a mixture of 50 mM glucose and 150 mM sucrose. To obtain complete solubilization of the polyelectrolyte, we add the stoichiometric amount of HCl on the basis of NH_2 amount (final pH around 3.4). The solution is placed under constant stirring for one night at room temperature, until complete solubilization, and filtered on a calibrated 0.2 μm membrane before use.

Sucrose and D-*(+)-glucose* are purchased from Sigma-Aldrich and used as received. The solutions of sucrose and glucose in water are prepared at different concentrations depending on the experiments.

Unilamellar giant vesicles (GUVs) are prepared from DOPC, using the standard electroformation method:[41] 20 μL of a solution of DOPC (2 mg/mL) is deposited on each indium tin oxide (ITO) plate. Hydration under an ac field is made in 2.5 mL of a 200 mM solution of sucrose.

Small unilamellar vesicles (LUVs) (for ζ-potential measurements) are prepared from 2.5 mL of giant vesicles in suspension in a 200 mM solution of sucrose directly obtained from the electroformation by extrusion on 0.2 μm filters and then dilution in the same volume of a filtered solution of 50 mM glucose and 150 mM sucrose. The extruded LUVs, 200 ± 10 nm in diameter, encapsulate a 200 mM solution of sucrose and are suspended in an external glucose/sucrose mixture to allow light scattering studies. It was established that LUVs prepared in these conditions are unilamellar.[42]

GUVs were incubated in chitosan solution for direct observation by optical microscopy. Unlike Henriksen et al.,[29] who add the liposome suspension into the chitosan solution, we chose to add chitosan in the vesicle solution as follows: 4.6 mL of a dilute giant vesicles suspension is incubated for 1 h at room temperature with 150 μL of chitosan solution prepared as explained previously. The specific amount of chitosan to be added is determined thanks to ζ-potential experiments detailed later in this paper. The external solution consists of a mixture of 50 mM glucose and 150 mM sucrose solutions in order to be the same experimental conditions as for ζ-potential studies of LUVs.

*Poly(*L*-lysine)-coated glass slides are used for adhesion study.* Poly(L-lysine) is purchased from Sigma-Aldrich and used as received to prepare a 1 mg/mL solution in water. Glass slides are immersed in a "piranha" solution ($^1/_3$ H_2O_2 + $^2/_3$ H_2SO_4) for 1 h and washed successively with water and methanol before incubation in the 1 mg/mL poly(L-lysine) solution for 1 h.

Methods. *ζ-Potential and dimension measurements on LUVs* are performed with a commercial zetasizer (NanoZS, Malvern, France). Electrophoretic mobilities of liposomes are measured using the zetasizer. The mobility (μ) is converted into a ζ-potential using the Smoluchowski relation ($\mu = \epsilon\epsilon_0\zeta/\eta$, where η and $\epsilon\epsilon_0$ are the viscosity and the permittivity of the external solution, respectively). The particle radii are controlled in situ by light scattering. For each ζ-potential measurement, the following protocol is repeated: a given volume of the chitosan solution is added to the liposome suspension. After homogenization, 1 mL of this mixture is injected in the zetasizer nanocell; the ζ-potential of the solution is measured at 20 °C. After each measurement, the whole solution is collected from the zetasizer nanocell and reintroduced into the bulk solution (to keep a nearly a constant volume of solution) before the addition of the next volume of chitosan solution. Those steps are repeated as many times as necessary. ζ-Potential measurements were performed in a mixture of 150 mM sucrose and 50 mM glucose solution and with the following lipid concentrations: for experiments in the presence of HCl and NaCl, we use a suspension of LUVs obtained with a DOPC concentration equal to 0.006 mg/mL, which corresponds to [DOPC] equal to 3.8×10^{-6} M in the external leaflets if we assume external and internal leaflet areas are approximately the same. As far as experiments in the presence of chitosan (Mw = 225 000) are concerned, the DOPC concentration is equal to 0.016 mg/mL, which corresponds to a molar concentration of DOPC equal to 10.18×10^{-6} M in the external leaflets. In the case of experiments made with chitosan of Mw = 50 000, mass DOPC concentration is equal to 0.015 mg/mL, which corresponds to a molar concentration of DOPC equal to 9.5×10^{-6} M in the external leaflets.

Adhesion. Poly(L-lysine)-coated glass slides are dried under argon flow and Secure-Seal hybridization chambers (purchased from Sigma) are stuck onto their surfaces in order to obtain observation chambers of 500 μL. The suspension of giant vesicles treated with chitosan is injected in the chamber (filled with a solution of 200 mM glucose) and we observe the sedimentation and the contact of the vesicles with the glass sheet.

Osmotic Deflation. To apply controlled osmotic pressure steps on the giant vesicles, we use a "homemade" device (Figure 2). It consists of five circular chambers, one central and four side ones, overlapping each other, so that each side chamber is connected to the central one, but independent from the others. The fluid in the side chambers (i, ii,

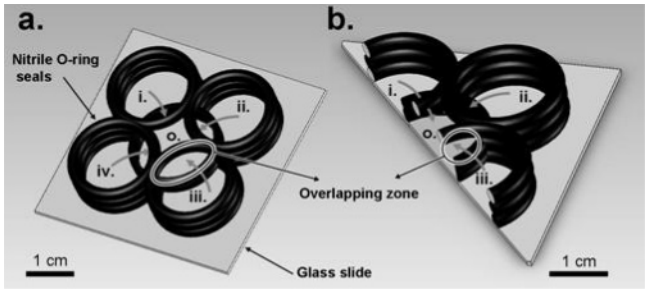

Figure 2. Experimental setup used to observe GUVs under external stresses (salts, pH, or glucose shocks): (a) top view, (b) cross section.

Figure 3. A sedimented DOPC GUV on a glass substrate before and during incubation with chitosan at pH = 5 in the absence of external salt. Scale bars represent 5 μm.

iii, and iv) is allowed to diffuse in the central zone (0) through the overlapping zone. Each chamber has a volume of roughly 1 mL. We successively fill the central chamber with 400 μL of 200 mM glucose, 200 μL of the giant vesicle suspension under study, and 400 μL of 200 mM glucose to reach a final volume of 1 mL. In this way, the external solution is nearly 200 mM glucose, allowing sedimentation of GUVs (which encapsulate a 200 mM sucrose solution) and creating a variation of optical index between inner and outer media of vesicles required for the phase-contrast microscopy observation. We close the chamber with a cover glass (to correct the curvature of fluid/air interface) and wait 30−40 min for vesicles to sediment on the glass slide. Osmotic deflations were performed with solutions of glucose, NaCl, or HCl at different concentrations. Concentrations of solutions injected in the side chambers are chosen according to the osmotic pressure, pH, and salt shocks (respectively controlled by glucose, HCl, and NaCl concentrations) we want to apply on the vesicles in the central chamber. Osmotic stress is determined on the basis of external and internal osmolalities characterized by the reduced volume ν, defined as the ratio between the volume of the deflated object and the volume of the initial spheric vesicle of the same surface. The ν value is calculated in a first approximation as the ratio of initial glucose concentration (200 mM) over the actual external glucose concentration.

Optical observations are made using a phase-contrast inverted microscope (Olympus CKX41) and a numerical camera (AVT MarlinF080B). Image analysis is performed using NIH Image J1.34s software (freely available at http://rsb.info.nih.gov/ij/).

Results and Discussion

Chitosan−Giant Vesicles: Observation by Optical Microscopy. We have first observed the behavior of the giant vesicles in the presence of the solution of chitosan used for incubation as a function of the time. Figure 3 presents a vesicle before and during incubation. After 70 min of incubation, we do not observe any bursting or shape modification of the vesicle. This result indicates either that no interaction occurs between chitosan and the membrane of the vesicle or that interaction exists but does not alter the shape of the object. Taking this result into account, the interaction of chitosan with liposomes (LUVs) was first investigated. Due to the acidic pH of the chitosan solution, the first step of the study was to investigate the influence of pH and ionic concentration on LUV characteristics (charge and stability) in the absence of chitosan.

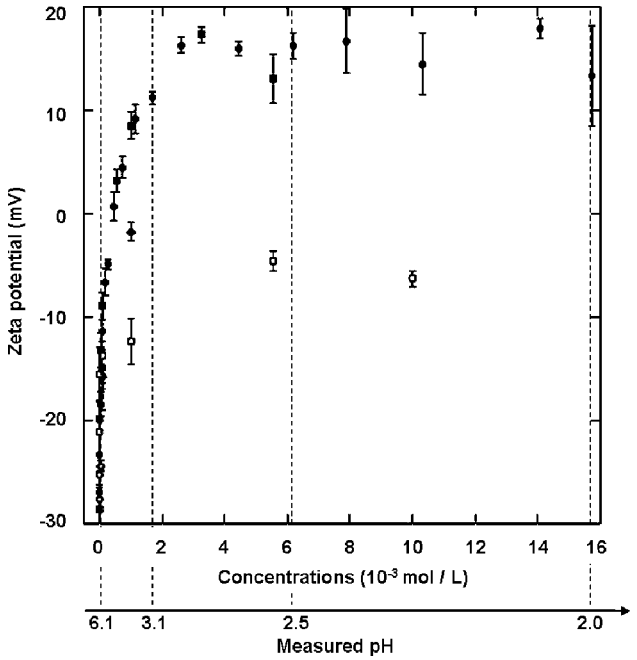

Figure 4. ζ-Potential of DOPC LUVs as a function of added HCl (solid circles and squares) and NaCl (open circles and squares) for different series of measurements in the same experimental conditions. A pH scale is joined to further characterize HCl additions.

Influence of pH and Salt Concentration on Naked LUVs. Taking into account that pH varies when we add successive amounts of chitosan solution, it is necessary to be able to discriminate between pH and chitosan effects. Therefore, we first observed pH effects on the ζ-potential of "naked" liposomes in a large range of pH, i.e., 6.0 > pH > 2.5. ζ-Potential is measured to be negative (−25 mV) at the initial pH = 6.0. Such a negative potential for DOPC LUVs was already reported in the literature.[43] This negative potential was assumed to result from lipid degradation during the rehydration phase, and this phenomenon is amplified by the active process of electroformation. When the pH is decreased by addition of HCl, the ζ-potential goes to zero at pH = 4, becomes positive, and finally reaches a constant value of +16 ± 1 mV at pH = 3.0 (see Figure 4). In fact, increasing the H_3O^+ concentration represses the dissociation of the phosphate acid group. The positive contribution of the quaternary amino group becomes then predominant. The large variation of ζ-potential is observed in a range of proton molar concentration up to 5×10^{-4} M, which is negligible in front of the 200 mM concentration of the external glucose/sucrose mixture; then the influence on the osmotic pressure remains negligible. In addition, for HCl and NaCl concentrations up to 5×10^{-3} M, the dimension of liposomes remain unchanged (diameter around 200 nm), which confirms that liposomes do not burst nor change their dimension.

It is important to differentiate between protonic and ionic concentration influence on the ζ-potential. Therefore, we repeated the same experiments with NaCl instead of HCl. Experimental results are also presented in Figure 4. The ζ-potential decreases in absolute value and levels at around −5 mV. A very large variation is observed up to 10^{-3} M NaCl, which is also low compared with the external glucose/sucrose concentration. The role of NaCl is completely different from that of HCl, which is much more efficient to modify ζ-potential going even to charge inversion. In the literature, molecular dynamics studies show that the presence of NaCl only affects the lateral orientation of phosphatidylcholine head groups of the external leaflet, resulting from the binding of sodium ions

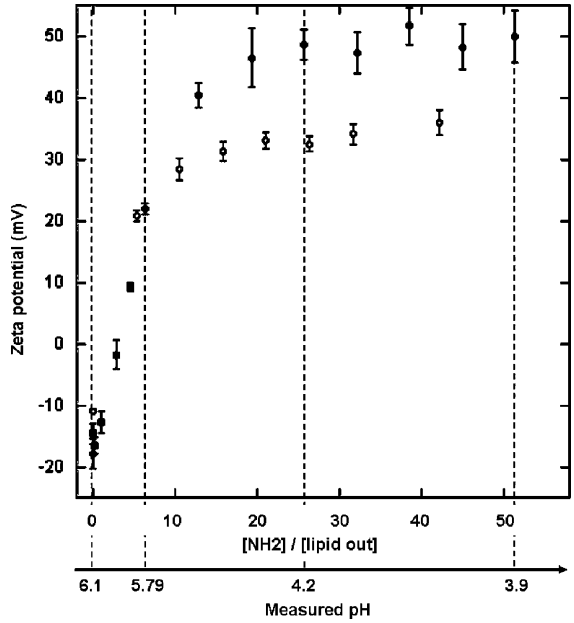

Figure 5. Variation of the ζ-potential as a function of the ratio between the amount of chitosan amino groups and DOPC groups in the external leaflet of LUVs for two different molecular weight chitosans: (solid circles and squares) Mw = 225 000 or (open circles and squares) Mw = 50 000. Measured pH are also indicated

in the carbonyl region of the leaflet and from the attractive interaction of Cl^- ions located in the aqueous phase close to the water−lipid interface.[44−46] NaCl is able to screen the electrostatic attraction between positively and negatively charged groups of each polar head.[47] This kind of mechanism is also involved in the salt effect on zwitterion solubility.[48,49]

Influence of Chitosan on ζ-Potential of LUVs. Finally, we performed the ζ-measurements for progressive additions of chitosan with two different molecular weights, namely 50 000 and 225 000. During the experiment, because of the addition of successive amounts of chitosan "mother" solution (at an initial pH of around 3.4) to the initial liposome solution (at pH = 6.0), the pH of the observed solution was found to vary between 6.0 and 3.9, thus allowing a perfect solubility of chitosan in all the experiments.[50,51] We observe a large variation of the ζ-potential with increasing the amount of added chitosan: from −18 to +49 mV (for Mw = 225 000) and +33 mV (for MW = 50 000) (see Figure 5). Taking into account that ζ-potential of naked liposomes only varies from −26 to +5 mV for pH ranging between 6.0 and 3.9, it is clear that these large variations can neither be attributed to the pH nor ionic concentration variations upon addition of this positively charged polyelectrolyte during the experiment; these results reveal the existence of a strong interaction between chitosan and lipid membrane.

At low chitosan concentrations (around two partially protonated glucosamines added per accessible polar heads of lipids), ζ-potential reaches zero and then becomes positive. In this range, we note a similar behavior for the two polymers with different molecular weights, which tends to prove that at these low concentrations of polysaccharide the adsorption is independent of the polymeric chains length and that charge inversion is obtained for the same amount of added chitosan. For higher concentration of chitosan, we observe a plateau, the value of which is higher for the long chain around +49 mV for Mw = 225 000 and +33 mV for Mw = 50 000. The results can be interpreted as follows: the first step (independent of Mw) consists of adsorption of chitosan flat on the membrane. Then, in a second step, we suggest that the polymer of higher molecular weight forms loops on the surface.

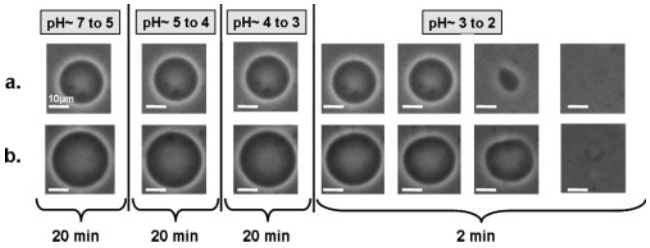

Figure 6. Naked GUVs of various sizes (a and b) as the pH decreases. They burst at pH = 2 after 2 min. Scale bars represent 10 μm.

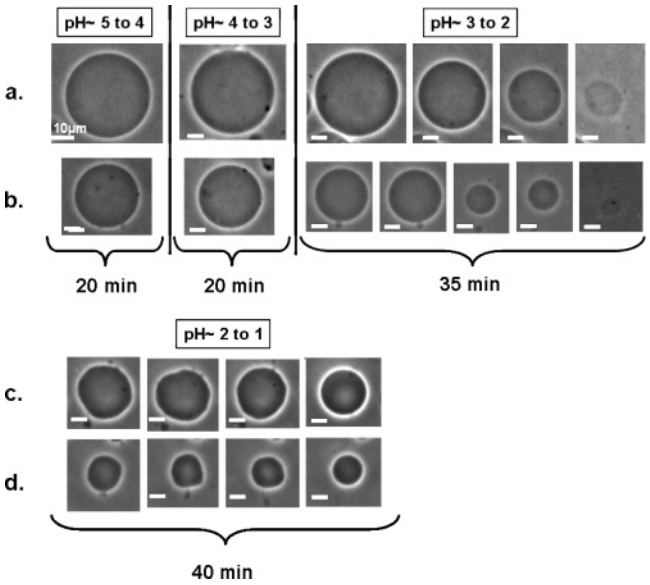

Figure 7. Decorated DOPC GUVs of various sizes (a−d) as a function of time for different pH values: (a and b) GUVs with chitosan burst at pH = 2 after 35 min; (c and d) GUVs that were not tracked during the previous pH shocks resist at pH = 1. The scale bars represent 10 μm.

We will now focus on GUVs. The behavior of DOPC GUVs either chitosan-decorated or not under different kinds of external stresses will be compared by direct optical microscopy observation. Interpretation of the behavior of giant vesicles will take into account data obtained for LUVs. In the following experiments, GUVs are incubated in a chitosan solution (Mw = 225 000) of 16.7 10^{-3} mg/mL, which corresponds to the beginning of the plateau of ζ-potential observed in Figure 5, where liposomes are highly positively charged.

Influence of pH on Naked and Chitosan-Decorated GUVs. The positive charge of chitosan depends on the pH, and our first concern was to study the stability of the chitosan-decorated vesicle (initial pH of nondecorated vesicle suspension is 6.0) as a function of pH. To directly detect the structural consequences of the addition HCl on the micrometric scale, we observed giant vesicles with phase-contrast microscopy as a function of the pH (obtained by HCl addition in the experimental device described in Figure 2). In order to avoid a large disturbance in the observation chamber, controlled amounts of acid are allowed to diffuse slowly to the observed vesicles. The amounts of added HCl in 200 mM glucose solution are chosen to reach a calculated pH successively equal to 5, 4, 3, and 2, and we wait several minutes in order to obtain a homogeneous concentration in the observation chamber.

Two similar experiments were performed: the first one, on nondecorated (referred to as naked) GUVs (Figure 6) and the

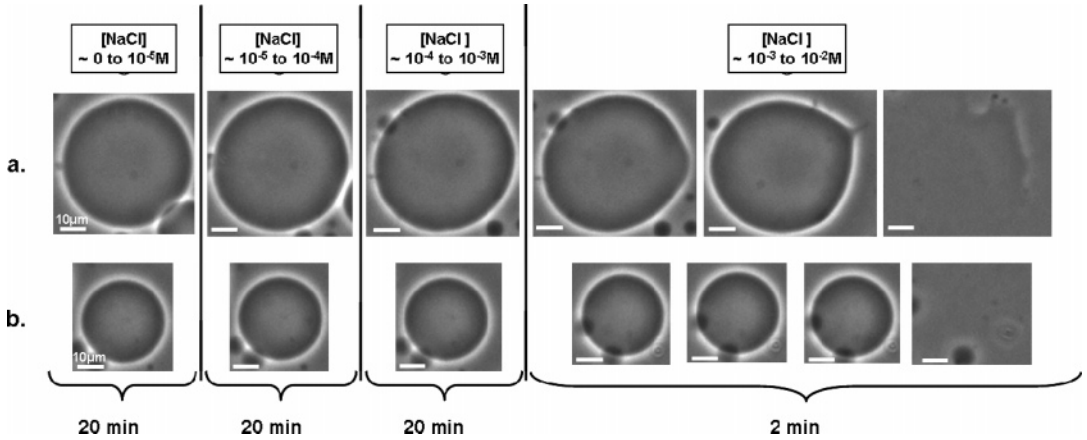

Figure 8. Naked GUVs of various sizes (a and b) as a function of NaCl concentration at initial pH = 5. The scale bars represent 10 μm.

second one on vesicles decorated with chitosan (Figure 7). In the initial state all the vesicles are quasispherical. Figure 6 shows three sequences of pictures of naked GUVs after injection of HCl.

The first column of Figure 6 shows the quasispherical vesicles at the osmotic equilibrium in a solution of 200 mM glucose. Although above pH = 4 we note no modification of the vesicle's shape, for 4 > pH > 3, the vesicles fluctuate slightly, which can be explained by a very weak osmotic deflation due to HCl concentration. At 3 > pH > 2, we observe large membrane thermal fluctuations, and all the vesicles burst after 2 min. In this range of pH, dissociation of the phosphate group is repressed and the lipid becomes positively charged due to the presence of the quaternary ammonium. The instability of the membrane may be ascribed to repulsion between the positive charges of head groups. In addition, a contribution of osmotic pressure may also contribute to disruption of the membrane. The delay before bursting may be attributed to the diffusion time, i.e., the time for HCl to reach the observed vesicles. The initial vesicle sizes do not influence the tendency to lyse.

This experiment was then repeated with decorated vesicles (see Figure 7). Both experiments are strictly made under the same conditions, and vesicles are observed at the same distance from the injection zone. Above pH = 3, we observe the same behavior as for naked vesicle. At 3 < pH < 2, large fluctuations occur, too, but it takes more than 30 min for some of the vesicles to burst. Taking into account the strictly similar experimental conditions used for naked and decorated vesicles, the greater delay before bursting observed for decorated GUVs may be attributed to the stabilization resulting from the presence of chitosan. While some of the decorated GUVs burst at 3 < pH < 2, a large percentage of them never burst, even at 2 < pH < 1. They first exhibit thermal fluctuations and then get stabilized under the shape of a sphere of smaller diameter. These results show further evidence of the vesicles decoration. We stress the amazingly large range of pH stability of chitosan-decorated vesicles, which evidence both electrostatic and hydrophobic attractions.

While some of the vesicles burst at pH ~ 2, as described just before, we observe that a large percentage of them remain stable at pH ~ 1. This difference in stability may be ascribed to a polydispersity in decoration degree, the highest ones corresponding to the highest stability. Nevertheless, in these experiments, pH was varied by successive addition of HCl, and our concern was then to show that the observed effects were really due to pH and not to an ionic effect. That is the reason why we studied the effects of salt shock.

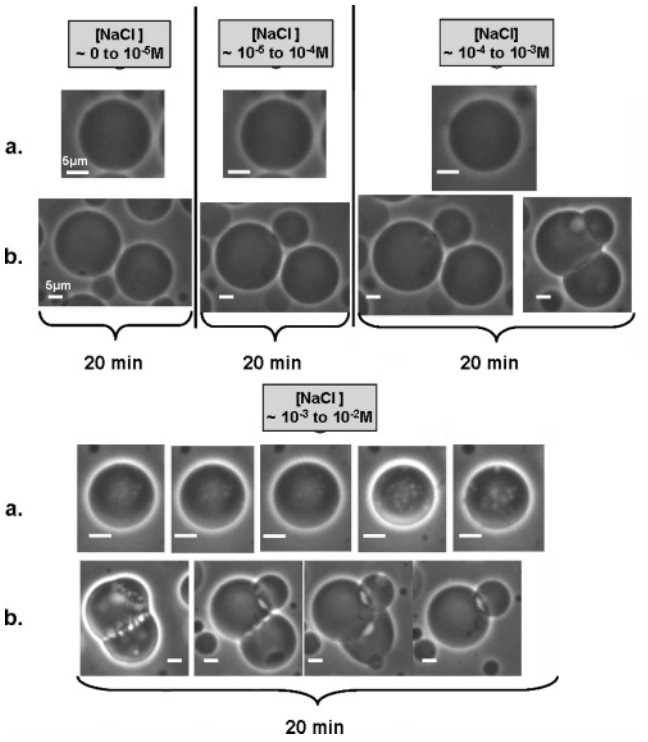

Figure 9. Decorated DOPC GUVs of various sizes (a and b) as a function of time for different NaCl concentrations (up to 10^{-2} M) at initial pH = 5. (a) Single vesicle and (b) aggregate of vesicles. The scale bars represent 5 μm.

Influence of Salt on Naked and Chitosan-Decorated GUVs. The same experiments as previously were performed substituting NaCl for HCl, in order to modify the ionic concentration instead of pH, on naked vesicles (Figure 8) and on vesicles decorated with chitosan (Figure 9).

As far as naked vesicles are concerned, we observe the same behavior of the vesicles as a function of HCl and NaCl concentration up to 10^{-2} M. This indicates that no difference is observable between salt and pH effects on the stability of giant vesicles, while on LUVs, ζ-potential shows different trends at concentrations $>10^{-3}$ M (Figure 4). Bursting of naked vesicles at higher concentrations of NaCl ($\approx 10^{-2}$ M) may be attributed to the combined effects of external osmotic pressure and ionic screening. Concerning the behavior of the decorated vesicles (Figure 9), results are fully different if compared to those obtained as a function of pH. No bursting occurs, but we can observe aggregation of vesicles when they are close together in the observation chamber. We can note that no aggregation

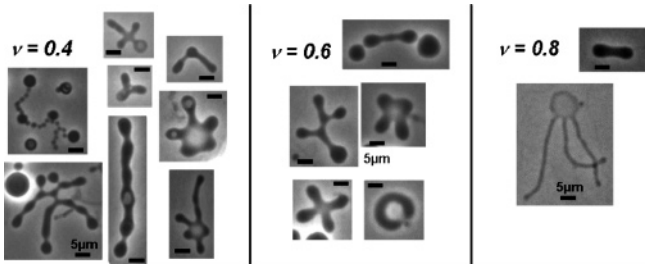

Figure 10. Osmotic deflation of chitosan-decorated DOPC GUVs induced by increase of the outer glucose concentration. Complex shapes were obtained for the different reduced volumes: 0.4, 0.6, and 0.8. The scale bars represent 5 μm.

process is observed by decreasing the pH due to electrostatic repulsion between the highly charged vesicles (Figure 7).

The first conclusion is that salt and pH effects on decorated vesicles are very different. Bursting of vesicles upon pH, when occurring in the range of 3 > pH > 2, can be attributed to both the lowering of chitosan adsorption due to its protonation and the decreasing of negative charge of the lipid phosphate group.[52] Addition of NaCl causes membrane aggregation. Such effects of monovalent salt are reported in the literature[53] and ascribed to a screening charge effect. This behavior may be related to the decrease of ζ-potential in absolute value, which results in an instability of the charged vesicle dispersion due to the screening of the long-range electrostatic repulsion.[54]

The interaction of chitosan with vesicles being proved, it was of interest to study the role of this decoration on the behavior of GUVs under external stresses such as osmotic pressure imposed by glucose gradient and adhesion on charged substrate.

Influence of Chitosan Decoration on the Behavior of GUVs under Osmotic Pressure. To investigate the effect of osmotic pressure, the glucose concentration of the external solution was stepwise increased, leading to a calculated reduced volume ν down to 0.4. The shape evolutions of several of chitosan-decorated vesicles submitted to the osmotic deflation are observed. Two kinds of phenomena occur: some vesicles remained spherical while shrinking, as detailed by Boroske et al.,[55] while others exhibited a large panel of complex shapes. Some of the complex shapes observed are presented in Figure 10. They present similarities with numerous theoretical and experimental shapes reported in the literature, like deflated shapes of fluid vesicles with a polymer chain anchored on the membrane[18] or shapes of lipid−cholesterol vesicles[56] or of vesicles exhibiting area asymmetry[57] associated with a surface area difference. Complex shapes can be described by different models involving either area difference elasticity (ADE)[57] or combining[19,20] the Helfrich curvature elasticity theory for fluid membranes[58] and the self-consistent field theory (SCFT). Complex and spherical shapes are observed simultaneously. We stress that in the present study, contrary to what is generally reported in the literature, spherical shrinkages are not isolated events for decorated vesicles: a large number (more than half of the objects) of vesicles experience a spherical deflation. Figure 11a presents a typical spherical deflation of a decorated vesicle, observed for calculated reduced volume $\nu = 1$, 0.8, 0.6, and 0.4. Figure 11b presents the variation of the dimensionless parameter $(r(t)/r_0)^3$, with r being the radius of the vesicle at a given time and r_0 the initial radius of the vesicle (i.e., before the first volume deflation), as a function of the predicted reduced volume ν. Each point of Figure 11b corresponds to the shape of the same number in Figure 11a. From points 1−4 of Figure 11b, $(r(t)/r_0)^3$ first decreases, passing through intermediate states 2 and 3 to progressively stabilize as state 4, which involves

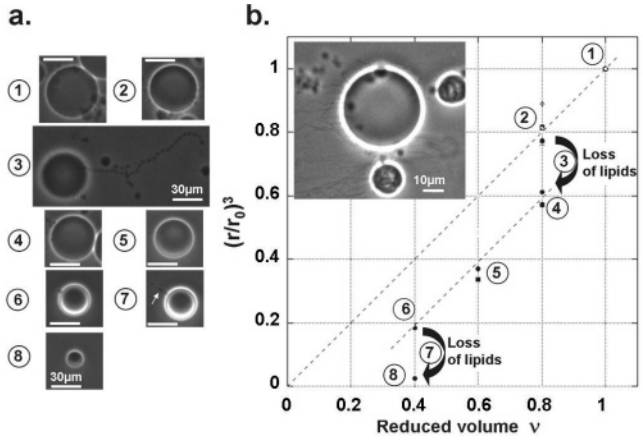

Figure 11. Osmotic deflation in glucose excess for chitosan-decorated DOPC GUVs: (a) pictures of the spherical deflation shapes of a decorated vesicle, the numbers of the pictures refer to those written in panel b. The scale bars represent 30 μm. (b) Variation of $(r/r_0)^3$ as a function of the calculated reduced volume ν for the spherical deflation of ten vesicles and (inset) a vesicle exhibiting lipid tubes while remaining spherical during the experiments for a reduced volume of 0.8. The scale bars represent 10 μm.

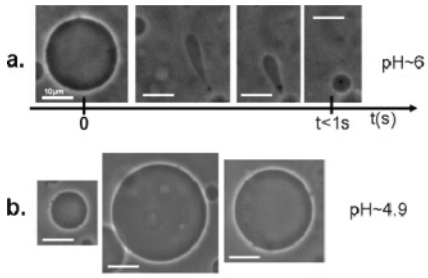

Figure 12. Behavior of DOPC GUVs in the presence of a glass substrate treated with poly(L-lysine): (a) a naked DOPC GUV sediments at pH ∼ 6, adheres, and bursts very quickly due to the strong adhesion. (b) Pictures of three different chitosan-decorated GUVs observed 30 min after the contact with the substrate; all the vesicles are intact. The scale bars represent 10 μm.

loss of lipid imposed by the decrease of membrane area. The same process occurs between states 5 and 8. The large deflation of vesicle is associated with a release of a large amount of lipids in the outer medium under the form of tubes and a pearl necklace (see picture 3 in Figure 11a). Our results confirm the interpretation of Boroshe et al.,[55] who explained spherical deflation by the formation of tubes of lipids attached to the sphere. Simultaneous observation of spherical and deflated complex shapes may be attributed to different degrees of decoration.

Influence of Chitosan Decoration on the Behavior of GUVs under Adhesion on a Positively Charged Substrate. Our aim is now to observe the effect of the chitosan decoration on GUV adhesion on a poly(L-lysine)-treated substrate, which is positively charged in acidic medium. A comparative study between naked vesicles and chitosan-coated vesicles (Figure 12) was performed. In the case of naked negatively charged vesicles at an effective pH around 6.0, they sediment, adhere with the positively charged substrate, and burst as soon as they come in contact with the substrate, due to the increase in the membrane tension (Figure 12a). On the contrary, chitosan-coated vesicles do not burst, even after 30 min (Figure 12b), and under gentle flow they start to move. It is proof that there is no adhesion between GUVs decorated with chitosan and positively charged substrate. These results give further evidence of the strong interaction of chitosan with DOPC vesicles. The absence of

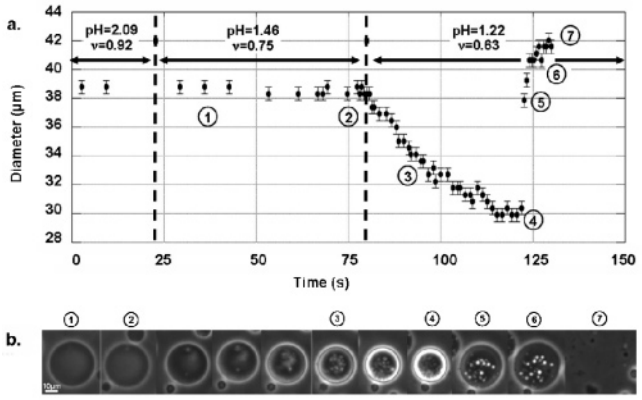

Figure 13. Behavior of decorated DOPC GUVs in the presence of a glass substrate treated with poly(L-lysine) as a function of the pH: (a) Variation of the diameter of the vesicle for pH < 2.10 as a function of the time and (b) evolution of a decorated DOPC−chitosan GUV in the pH range 1.5 > pH > 1.2. The scale bars represent 10 μm.

adhesion is attributed to electrostatic repulsion between positively charged substrate and chitosan−GUVs.

Now we try to highlight the pH effect on the interaction between the chitosan-decorated vesicle and the positively charged substrate (poly(L-lysine)). In order to test the feasibility to control adhesion, we chose to study the behavior of decorated vesicles sedimenting on a poly(L-lysine) substrate when the pH progressively varies. Figure 13a presents the evolution as a function of time of GUV diameter upon successive HCl additions. Indicated pHs correspond to the predicted value at equilibrium. Figure 13b shows decorated vesicles corresponding to the states of same numbers as in Figure 13a.

From pH = 5.0 to 3.3 (not represented in the Figure 13a), GUV diameters do not change ($\nu \approx 1$). At 3 > pH > 1.5, we only observe a small deflation resulting from osmotic pressure change (due to the variation of HCl concentration) (Figure 13a). GUV shapes remain spherical (Figure 13b, pictures 1 and 2).

At pH = 1.2, we observe the following evolution as a function of time: first a sharp decrease of the diameter [Figure 13a; related vesicles are presented Figure 13b (pictures 2−4)], followed by a sudden size increase, leading to a final diameter larger than the initial one (Figure 13b, pictures 4−7), and finally the bursting of the vesicle. The spherical deflation occurs with formation of small daughter vesicles (Figure 13b). This specific behavior (instead of formation of lipid tubes) may be due to the presence of the positively charged substrate causing electrostatic repulsion and may be considered as a first step before adhesion (states 5 and 6 in Figure 13a and related pictures in Figure 13b). This possible adhesion may be related to both the lowering of chitosan adsorption due to its protonation and the decreasing of negative charge of the lipid phosphate group,[52,59] as already proposed to explain liposome instability.

Conclusion

We succeeded in decorating DOPC LUVs and GUVs (considered as simple model for living cells) with positively charged chitosan in acidic medium. Decoration strongly enhances the vesicles' stability against salt (NaCl) and pH shocks, revealing strong interactions between chitosan and the lipid bilayer, which are both of electrostatic and hydrophobic origin. Nevertheless, in intermediate range of pH, long-range electrostatic interactions are predominant. Sorption of chitosan on vesicles was shown to play a crucial role in their self-interaction, in their interaction with charged substrates, and in their behavior under osmotic pressure controlled by glucose concentration. These stabilized vesicles hold promise as in vivo resistant protective capsules.

Acknowledgment. We would like to thank the University of Konstanz and the International Research Training Group (IRTG) for their financial support.

References and Notes

(1) *Structure and Dynamics of Membranes, Handbook of Biological Physics*; Lipowsky, R., Sackmann, E., Eds.; Elsevier science B. V.: Amsterdam, 1995; Vols. 1A and 1B.
(2) Photos, P. J.; Bacakova, L.; Discher, B.; Bates, F. S.; Discher, D. E. *J. Controlled Release* **2003**, *90*, 323−334.
(3) Tong, W.; Gao, C.; Möhwald, H. *Macromolecules* **2006**, *39*, 335−340.
(4) Torchilin, V. P. *Nature Rev.* **2005**, *4*, 145−160.
(5) Malmsten, M. Protein adsorption in intravenous drug delivery. In *Biopolymers at Interfaces*; Malmsten, M., Ed.; Dekker: New York, 2003.
(6) Malmsten, M. *Soft Matter* **2006**, *2*, 760−769.
(7) Gregoriadis, G. *Int. J. Pharm.* **1998**, *162*, 1−3.
(8) Rui, Y.; Wang, S.; Low, P. S.; Thompson, D. H. *J. Am. Chem. Soc.* **1998**, *120*, 11213−11218.
(9) Drummond, D. C.; Meyer, O.; Hong, K.; Kirpon, D. B.; Papahadjopoulos, D. *Pharm. Rev.* **1999**, *51*, 691−743.
(10) Templeton, N. S.; Lasic, D. D. *Mol. Biotechnol.* **1999**, *11*, 175−180.
(11) Cevc, G.; Blume, G. *Bioch. Biophys. Acta* **2001**, *1514*, 191−205.
(12) Gregoriadis, G.; Bacon, A.; Caparros-Wanderley, W.; McCormack, B. *Vaccine* **2002**, *20* (suppl. 5), B1−B9.
(13) Fattal, E.; Couvreur, P.; Dubernet, C. *Adv. Drug Delivery Rev.* **2004**, *56*, 931−946.
(14) Souza, S. M. B.; Oliveira, O. N.; Scarpa, M. V.; Oliveira, A. G. *Colloids Surf. B* **2004**, *36*, 13−17.
(15) Martina, M. S.; Fortin, J. P.; Menager, C.; Clement, O.; Barratt, G.; Grabielle-Madelmont, C.; Gazeau, F.; Cabuil, V.; Lesieur, S. *J. Am. Chem. Soc.* **2005**, *127*, 10676−10685.
(16) Frezard, F.; Schettini, D. A.; Rocha, O. G. F.; Demicheli, C. *Quim. Nova* **2005**, *28*, 511−518.
(17) Singer, S. J.; Nicolson, G. L. *Science* **1972**, *175*, 720−731.
(18) Tsafrir, I.; Sagi, D.; Arzi, T.; Guedeau-Boudeville, M.-A.; Frette, V.; Kandel, D.; Stavans, J. *Phys. Rev. Lett.* **2001**, *86*, 1138−1141.
(19) Wang, J.; Guo, K.; Qiu, F.; Zhang, H.; Yang, Y. *Phys. Rev. E* **2005**, *71*, 4, 041908.
(20) Sun, M.; Qiu, F.; Zhang, H.; Yang, Y. *J. Phys. Chem. B* **2006**, *110*, 9698−9707.
(21) Hiergeist, C.; Lipowsky, R. *J. Phys.* **1996**, *II 6*, 1465−1481.
(22) Kim, Y. W.; Sung, W. *Phys. Rev. E* **2001**, *63*, 041910−419105.
(23) Breidenich, M.; Netz, R. R; Lipowsky, R. *Eur. Phys. J. Lett.* **2000**, *49*, 431−437.
(24) Charrois, G. J. R.; Allen, T. M. *Bioch. Biophys. Acta* **2003**, *1609*, 102−108.
(25) Sapra, P.; Allen, T. M. *Prog. Lipid Res.* **2003**, *42*, 439−462.
(26) Rinaudo, M. *Prog. Polym. Sci.* **2006**, *31*, 603−632.
(27) Kas, H. S. *Microcapsules* **1997**, *14*, 689−711.
(28) Mertins, O.; Borda Cardoso, M.; Raffin Pohlmann, A.; Pesce da Silveira, N. *J. Nanosci. Nanotechnol.* **2006**, *6*, 1−7.
(29) (a) Henriksen, I.; Vagen, S. R.; Sande, S. A.; Smistad, G.; Karlsen, J. *Int. J. Pharm.* **1997**, *146*, 193−204. (b) Henriksen, I.; Smistad, G.; Karlsen, J. *Int. J. Pharm.* **1994**, *101*, 227−236.
(30) Illum, L.; Farraj, N. F.; Davis, S. S. *Pharm. Res.* **1994**, *11*, 1186−1189.
(31) Elbert, D. L.; Hubbell, J. A. *Annu. Rev. Mater. Sci.* **1996**, *26*, 365−294.
(32) Richardson, S. C.; Kolbe, H. V.; Duncan, R. *Int. J. Pharm.* **1999**, *178*, 231−243.
(33) Venter, J. P.; Kotzé, A. F.; Auzély-Velty, R.; Rinaudo, M. *Int. J. Pharm.* **2006**, *313*, 36−42.
(34) Strand, S. P.; Danielsen, S.; Christensen, B. E.; Varum, K. M. *Biomacromolecules* **2005**, *6*, 3357−3366.
(35) Strand, S. P.; Tommeraas, K.; Varum, K. M.; Ostgaard, K. *Biomacromolecules* **2001**, *2* (4), 1310−1314.
(36) Fang, N.; Chang, V.; Mao, H. Q.; Leong, K. W. *Biomacromolecules* **2001**, *2*, 1161−1168.
(37) Fang, N.; Chan, V. *Biomacromolecules* **2003**, *4*, 581−588.

(38) Fang, N.; Chan, V. *Biomacromolecules* **2003**, *4*, 1596−1604.
(39) Mertins, O.; Sebben, M.; Raffin Pohlmann, A.; Pesce da Silveira, N. *Chem. Phys. Lipids* **2005**, *138*, 29−37.
(40) Rinaudo, M.; Auzely, R.; Vallin, C.; Mullagaliev, I. *Biomacromolecules* **2005**, *6*, 2396−2407.
(41) Angelova, M. I.; Soleau, S.; Meleard, P.; Faucon, J.-F.; Bothorel, P. *Prog. Colloid Polym. Sci.* **1992**, *89*, 127−133.
(42) (a) Nayar, R.; Hope, M. J.; Cullis, P. R. *Biochim. Biophys. Acta* **1989**, *986*, 200−206. (b) Hope, M. J.; Bally, M. B.; Webb, G.; Cullis P. R. *Biochim. Biophys. Acta* **1985**,*812*, 55−65.
(43) Luisi, P. L.; Walde, P. *Giant Vesicle*; John Wiley & Sons: New York, 2002; pp 108−112.
(44) Gurtovenko, A. A. *J. Chem. Phys.* **2005**, *122*, 244902−244911.
(45) Rappolt, M.; Pabst, G.; Amenitsch, H.; Laggner, P. *Colloids Surf. A* **2001**, *183*, 3730−3742.
(46) Böckmann, R. A.; Hac, A.; Heimburg, T.; Grubmuller, H. *Biophys. J.* **2003**, *85*, 1647−1655.
(47) Sabin, J.; Prieto, G.; Ruso, J. M.; Hidalgo-Alvarez, R.; Sarmiento, F. *Eur. Phys. J. E* **2006**, *20*, 401−408.
(48) Lee, W. F.; Lee, C. H. *Polymer* **1997**, *38*, 971−979.
(49) Skouri, M.; Munch, J. P.; Candau, S. J; Neyret, S.; Candau, F. *Macromolecules* **1994**, *27*, 69−76.
(50) Rusu-Balaita, L.; Desbrières, J.; Rinaudo, M. *Polym. Bull.* **2003**, *50*, 91−98.
(51) Rinaudo, M.; Pavlov, G.; Desbrieres, J. *Int. J. Polym. Anal. Charac.* **1999**, *5*, 267−276.
(52) Baril, J.; Max, J.-J.; Chapados, C. *Can. J. Chem.* **2000**, *78*, 490−507.
(53) Roux, M.; Bloom, M. *Biochemistry* **1990**, *29*, 7077−7089.
(54) McLaughlin, S. *Annu. Rev. Biophys. Biophys. Chem.* **1989**, *18*, 113−136.
(55) Boroske, E.; Elwenspoek, M.; Helfrich, W. *Biophys J.* **1981**, *34*, 95−109.
(56) Hotani, H. *J. Mol. Biol.* **1984**, *178*, 113−120.
(57) Mui, B. L. S.; Döbereiner, H. G.; Madden, T. D.; Cullis, P. R. *Biophys. J.* **1995**, *69*, 930−941.
(58) Helfrich, W. Z. *Naturforsch* **1973**, *28c*, 693−703.
(59) Vasiliu, S.; Popa, M.; Rinaudo, M. *Eur. Polym. J.* **2005**, *41*, 923−932.

BM061227A